16th World Conference on Earthquake Engineering, 16WCEE 2017

Santiago Chile, January 9th to 13th 2017

Paper N° 126

Registration Code: S-D1461920075

IMPACT OF NON-LINEAR SOIL BEHAVIOR ON SITE RESPONSE AMPLITUDE

J. Régnier(1), H. Cadet(2), P-Y. Bard(3)

(1) *Phd, CEREMA Nice France, Julie.regnier@cerema.fr*
(2) *Phd, ADRGT, Grenoble, France, h.cadet@adrgt.org*
(3) *Phd, ISTerre/IFSTTAR, Grenoble, France,* pierre-yves.bard@ujf-grenoble.fr

Abstract

We present an extensive analysis of the quantitative impact of the non-linear soil behavior on site response at 174 sites of the Japanese KiK-net network. The nonlinear to linear site response ratio, $RSR_{NL\text{-}L}$ is calculated by comparing the surface / downhole Fourier spectral ratio for strong events and for weak events. 3 thresholds of surface PGA are tested to characterize the "strong events": 100, 200 and 300 cm/s^2, while weak events correspond to surface PGA in the range [0.1 – 25 cm/s^2]. This ratio exhibits a "typical shape"; with a low frequency part above 1 and a high frequency part generally below 1, separated by a transition zone around a site-dependent frequency labelled f_{NL} (characterized by $RSR_{NL\text{-}L} = 1$). The average maximum amplitudes of RSRNL-L are 1.4, 1.5 and 1.6, and the minimums 0.6, 0.5 and 0.5 for PGA thresholds 100, 200 and 300 cm/s^2 respectively, showing that non-linear soil behaviour results in significant site response modifications even for moderate PGA values of 100 cm/s^2.

Keywords: Nonlinear site response.

1. Introduction

For a given earthquake, the local variability in the seismic ground motions at different locations is mainly caused by lithological site effects. The resulting amplifications can go up to 10 and even 20 around resonance frequencies of sedimentary layers (Bard and Bouchon, 1985; Duval et al., 1996; LeBrun et al., 2001).

It is well recognized that the site effects can be significantly different for a strong event compared to small ones. The non-linear soil behavior of the sedimentary material can affect the seismic site response and consequently the surface ground motion (e.g. Beresnev and Wen, 1996). The main effects of non-linear soil behaviour are a degradation of its shear modulus and an increase in its attenuation properties. One of the main impacts of these changes on site response is a shift of the resonance frequencies towards lower values, together with a reduction in the associated amplifications. The modification of the site response can be significant (greater than 10%) even for moderate ground motions: Rubinstein, 2011 reports noticeable changes above a 35 cm/s^2 surface PGA threshold, while Régnier et al., 2013 indicate a 50 cm/s^2 downhole PGA threshold.

The empirical evidences for non-linear soil behaviour reported in the literature are: (1) an increase in the site response amplitude at relatively low frequencies, because of the frequency shift as mentioned by Frankel et al. (2002) and Régnier et al. (2013), (2) a decrease in the high frequency amplification over a relatively broad bandwidth for sites that do not exhibit pore pressure effects except (3), for sites that indicate liquefaction or cyclic mobility, where observation (2) is replaced by an increase of the site response at high frequencies (above 10Hz) (e.g. Bonilla et al., 2005; Frankel et al., 2002; Roten et al., 2013). The first evidence is as commonly reported in previous studies about non-linearity. For example, Beresnev and Wen (1996) reported a a decrease of the amplification from weak to strong motions (factor between 1.4 to 7), Field et al., (1997) showed a factor of 2 for site responses for all frequencies, Aguirre and Irikura (1997) showed a factor 4 decrease in the PGA amplification, Noguchi and Sasatani (2008) mentioned a factor of 2, and others also such as Bonilla et al., 2011; Satoh et al., 1995; Wen et al., 2011; Yu et al., 1993. reported similar observations. These studies used one or a few earthquake recordings over a restricted area. Conversely, recent large earthquakes such as the Great Tohoku 2011 event, which occurred close to well-instrumented area, offer a unique opportunity to study the non-linear soil behavior on a large dataset of strong ground motion recordings. Several recent studies compared vertical array recordings with the surface ground motion predicted with linear, equivalent linear and full non-linear methods, in view of better assessing the applicability domain of equivalent linear methods (Kaklamanos et al., 2013, 2015; Yee et al., 2013; Bolisetti et al., 2014; Zalachoris and Rathje, 2015a, 2015b; Kaklamanos and Bradley, 2015), together with the key parameters for characterizing the non-linear soil behaviour (Kaklamanos et al., 2013; Kim and Hashash, 2013).

The present paper is part of results published in Régnier et al (2016) and are builds on the previous results of Régnier et al (2013) which used all the strong motion recordings available over the period 1996-2009 from the well-known Japanese KiK-net accelerometric database, also including Tohoku earthquake in 2011 to compute empirical "borehole site responses" (i.e., surface / downhole Fourier spectral ratios) and to investigate the key soil and event parameters that influence the impact of soil nonlinear behavior on site response. In the present study, we add all strong motions (PGA at the surface > 100 cm/s^2) recorded from 2010 to 2014, and go one step further to provide a simple, first order quantification of the effects of non-linear soil behavior on site response. This is performed with an approach similar to the one followed by Field et al. (1997), through a frequency-dependent "modulation" factor derived from the comparison of the "non-linear" (i.e., high PGA) to the "linear" (i.e., low PGA) site response at every KiK-net site that experienced a surface PGA larger than 100 cm/s^2. The site response was estimated from the average surface-to-downhole Fourier spectral ratio, for different surface PGA values: lower than 25 cm/s^2 for the linear response, and higher than an a priori threshold value for the non-linear response, with three different values for this threshold: 100, 200 and 300 cm/s^2. The spectral shape of this ratio was analyzed for different subsets corresponding to different surface PGA thresholds.

2. Database and non-linear characterization

The Japanese Kiban–Kyoshin Network (KiK-net) used for this study is composed of 688 stations with surface and downhole accelerometers (Fujiwara et al., 2004). Most of the borehole seismic stations are located between 100 and 200 m depth. Among the KiK-net sites, 668 shear- and compressive-wave velocity profiles were collected from downhole logging measurements. Although most KiK-net stations are located on rock or thin sedimentary sites two thirds of the sites exhibit a Vs30 smaller than 550 m/s, representing softer sites with potentially large low frequency amplification.

The database used in Régnier et al. (2013) was composed of all the accelerometric data recorded between 1996 and 2009 with magnitudes (M_{JMA}) higher than 3, hypocentral depths and epicentral distances below 150 km, with the additional specific set of recordings from the great Tohoku earthquake. In the present paper, we add all strong events recorded from 2010 to 2014 with peak ground accelerations (PGA) higher than 50 cm/s^2 at depth, and without any criterion on distance. The data processing described in Régnier et al. (2013) was applied to this enlarged data set, with a focus on the site response estimated through the "borehole Fourier spectral ratio" (BSR in the following) between the surface and downhole recordings as defined in equation 1 (quadratic mean of the horizontal components).

$$BSR = \sqrt{\frac{EW_{surf}^2 + NS_{surf}^2}{EW_{Depth}^2 + NS_{Depth}^2}}, \quad (1)$$

Where, EW_{surf}, NS_{surf},, EW_{depth} NS_{depth}, are the Fourier spectra of the East-West, North-South components of the surface and down-hole recordings, respectively.

To analyze the effect of the non-linear soil behavior on site response, "weak" and "strong" motions were distinguished according to the surface PGA value. Weak motions, assumed to correspond to linear site response, were associated to PGA values from 0.1 to 25 cm/s^2, while "strong" motions, assumed to be affected by non-linear soil behavior, were associated to surface PGA values greater than some predefined threshold. Three different values were selected for this threshold: 100, 200 and 300 cm/s^2, which all ensure a large enough number of sites for statistical analysis. Among all KiK-net sites, the following subsets of sites that recorded at least two events with a PGA greater than the PGA threshold and at least two recordings with PGA between 0.1 and 25 cm/s^2 were obtained:

- Subset 1: 174 sites with PGA threshold value of 100 cm/s^2.
- Subset 2: 78 with PGA threshold value of 200 cm/s^2.
- Subset 3: 35 with PGA threshold value of 300 cm/s^2.

The non-linear modulation of the site response can be characterized by the logarithmic mean of the ratio between non-linear and linear BSRs, denoted hereafter RSR_{NL-L} (Ratio of Site Response, non-linear to linear). The ratio is calculated for each weak and strong motions couple, which makes $N_{strong(th)} \times N_{weak}$ ratios, which are then geometrically averaged. The RSR_{NL-L}, is therefore calculated for a given site as follows:

$$\log_{10}\left(RSR_{NL_{th}-L}\right) = \frac{1}{N_{strong(th)} \times N_{weak}} \left\lfloor \sum_{j=1}^{N_{strong(th)}} \sum_{i=1}^{N_{weak}} \log_{10}\left(\frac{BSR_j}{BSR_i}\right) \right\rfloor \quad (1)$$

With *j* the index on strong recordings (PGA higher than PGA threshold), *i* the index on weak recordings (PGA between 0.1 to 25 cm/s^2) and *th* the considered PGA threshold.

The RSR_{NL-L} represents the modification of the weak motion BSR resulting from non-linear soil behaviour. It is illustrated in Figure 1 for site IWTH14 and for a PGA threshold of 200 cm/s^2. The upper graph shows all BSRs with different PGA values according to the grey scale. The lower graph shows the corresponding computed empirical RSR_{NL-L}.

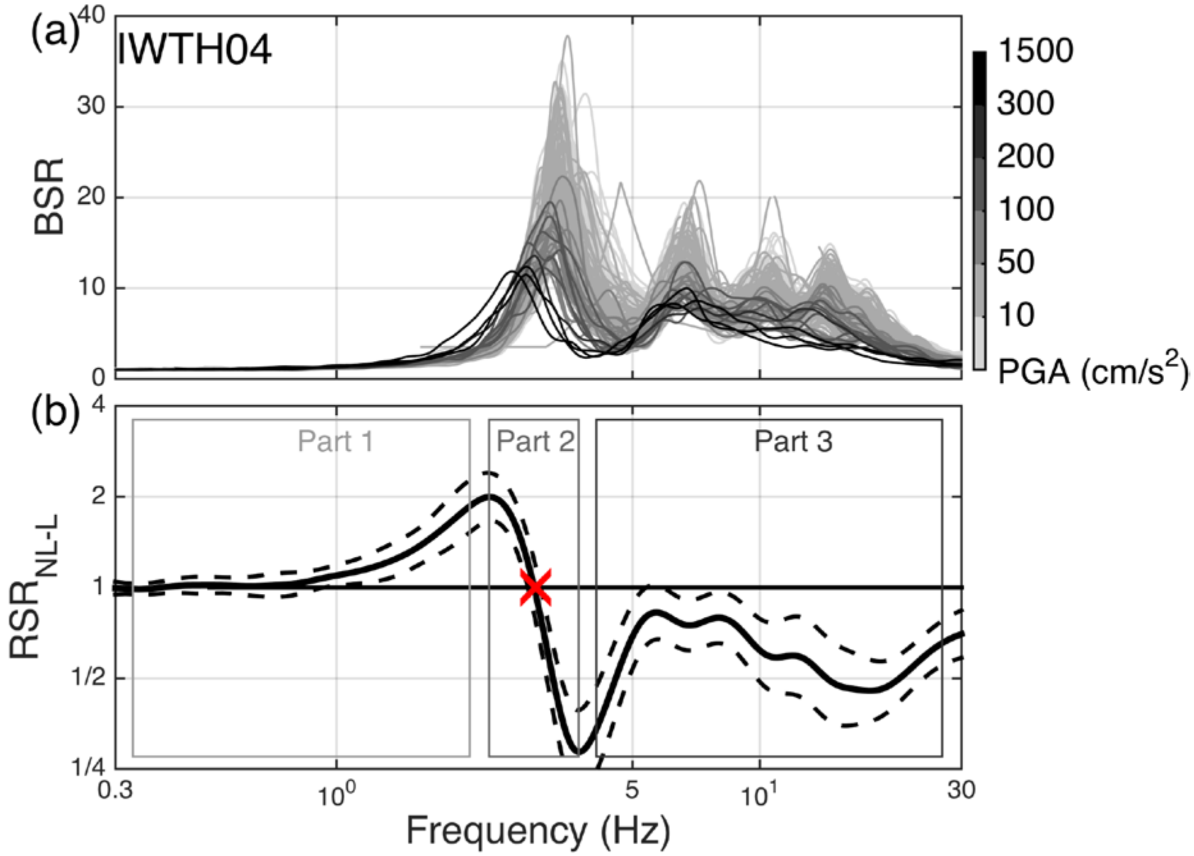

Fig. 1 – Illustration of the quantification of non-linear effects for one particular KiK-net site (IWTH04). (a) : surface/downhole spectral ratios, with a grey intensity corresponding to the surface PGA value in cm/s^2. (b): Non-linear frequency dependent modulation factor, RSR_{NL-L} derived from the comparison of large PGA site response (all those with a surface PGA exceeding 200 cm/s^2), to the weak motion response (derived from recordings with a surface PGA < 25 cm/s^2): thick black line = geometrical average, thin dashed lines = average ± one standard deviation; the f_{NL} value corresponds to the frequency where the average curve is becoming smaller than 1, is represented by the red cross.

As mentioned in different articles (e.g., Kokusho, 2004; Drouet, 2006; Cadet et al., 2012), the spectral ratio using the downhole recording as a reference (DWR) is biased by the so-called "depth effects" combining the frequency dependence of the free-surface effect, and the existence of destructive interferences at some specific frequencies.

For most sites, the RSR_{NL-L} curve exhibits the characteristic shape illustrated in Figure 1. It is composed of three main parts: i) Part 1 is characterized by an amplitude generally above 1 with a slow increase from 1 at (very) low frequency until a specific frequency that varies from one site to another; ii) Part 2 is an abrupt decrease of the amplitude from a maximum value above 1 to a minimum value below 1; and iii) Part 3 is characterized by a slow increase of the amplitude towards value close to 1 at high frequency. Within part 2, we define f_{NL} as the first frequency at which RSR_{NL-L} falls below 1. This parameter, which was previously proposed in Régnier et al. (2013), is site specific **and** PGA-threshold dependent. Indications on the range of f_{NL} values may be found in Table 1, which lists the average and standard deviation of f_{NL} for the three subsets. For Subset 1, f_{NL} could be picked automatically for 164 sites out of a total of 174 sites (for the remaining 10 sites, the non-linear soil behaviour is not significant enough for f_{NL} to be determined): it varies from 0.49 Hz to 15.7 Hz. For Subset 2, f_{NL} ranges from 0.85 Hz to 22.2 Hz and for Subset 3, f_{NL} varies from 1.4 Hz to 22.7 Hz.

Table 1 – Statistics on f_{NL} values for each subset of sites.

	Number of sites / f_{NL} values	arithmetic average f_{NL} (Hz)	f_{NL} range (Hz)	Standard deviation σ (Hz)
Subset 1 (PGA>100 cm/s^2)	**164**	**5.9**	*0.49-15.7*	*3.7*
Subset 2 (PGA >200 cm/s^2)	**76**	**6.0**	*0.85-22.2*	*3.9*
Subset 3 (PGA >300 cm/s^2)	**35**	**6.5**	*1.4-22.7*	*4.5*

The shape of the RSR_{NL-L} curve indicates that site response for strong motions is larger than that for weak motions for frequencies below f_{NL}, while it is the opposite for frequencies beyond f_{NL}. One major signature of non-linear soil behavior effects on site response is a shift of f_0 towards lower frequency range, caused by the decrease of the elastic soil properties (i.e., shear modulus) with increasing shear strain. In addition, the maximum increase and decrease of the site response from weak to strong motions are not symmetric around f_{NL}, the decrease part above f_{NL} being more pronounced. This observation provides a second evidence for the effects of non-linear soil behavior, consistent with an increase of the soil damping properties with increasing shear strain.

3. General trend for all sites

In order to provide a robust quantitative assessment of the impact of non-linear soil behaviour on site amplification, the RSR_{NL-L} from all sites were first combined together taking advantage of the generic shape of the RSR_{NL-L} curve displayed in Figure 1: for each site, the frequencies were normalized by the corresponding f_{NL} value, and the RSR_{NL-L} curves were plotted with a dimensionless frequency axis to compare the non-linear effect at the three different PGA thresholds values, we retained only the sites common to the 3 sites-subsets, defined earlier.

Over these 35 sites selected for comparison, the distribution of f_{NL} values ranges from 1.5 to 22 Hz, as illustrated in Figure 2. The f_{NL} values are in general larger than the f_0 values, especially for low frequency sites: the average f_{NL}/f_0 ratio is 2.2, 1.9 and 1.45 for subsets 1, 2 and 3, respectively. For 95% of the sites, f_0 is found to be a lower limit for f_{NL} values, as f_{NL} is larger than 0.8 f_0 for 95% of the sites. f_{NL} is stable among the three PGA thresholds values, except for 4 sites (IWTH20, MYGH05, NGN29, NIGH12), with lower values for the highest PGA threshold value of 300 cm/s^2. At those 4 particular, low frequency sites, only the higher modes / shallow layers are affected by non-linear effects for moderate motion (low PGA threshold values), whereas they also impact deeper layers and the fundamental frequency peak for larger PGA threshold values. This explains the decrease of f_{NL} with increasing PGA values.

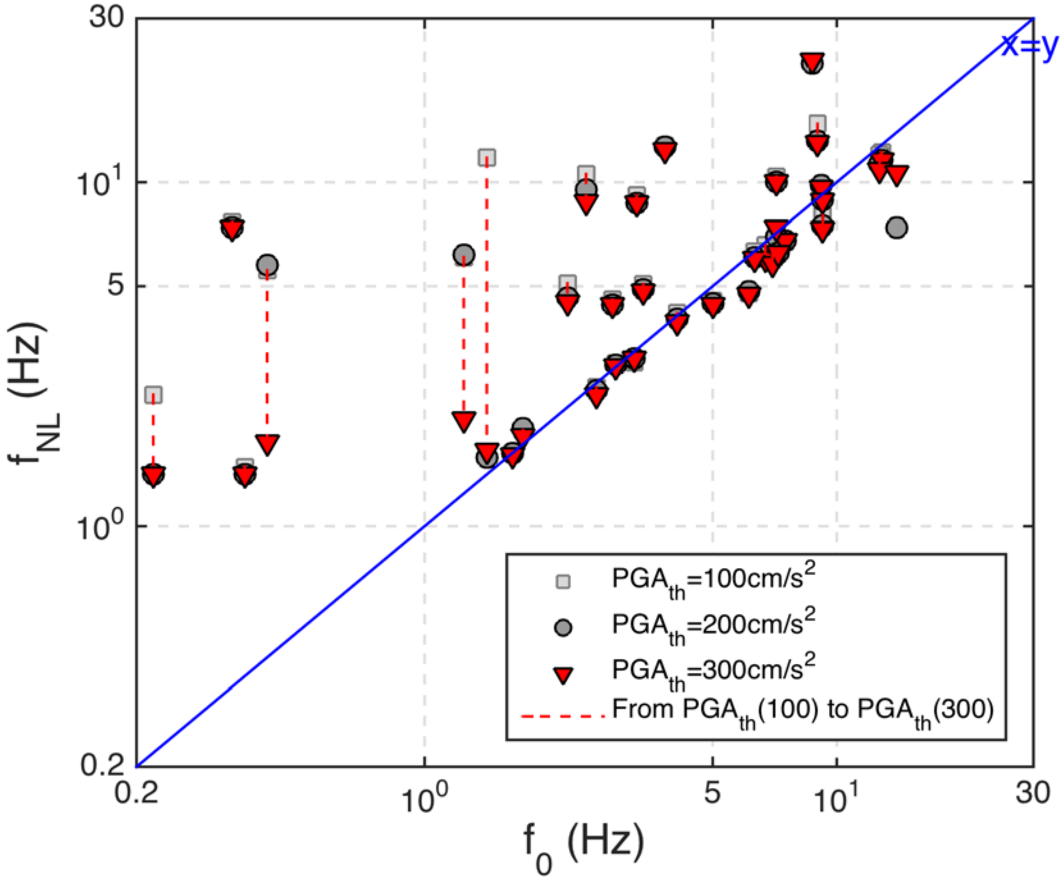

Fig. 2 –Distribution of f_{NL} values as a function of f_0 values for the 35 sites in subset 3. The different symbols correspond to the three different PGA thresholds.

The average and standard deviation values of the shifted (dimensionless frequency) RSR_{NL-L} curves are calculated for the three different subsets, and illustrated in Figure 3.

For the largest PGA threshold value of 300 cm/s^2 (subset 3), the non-linear soil response leads to an average low-frequency increase reaching a maximum value of 1.6 at a frequency about 0.76 times f_{NL}, while the average plus one standard deviation reaches a peak value of 2.7 around the same frequency. The transition part of the curve (Part 2), from over-amplification to under-amplification, extends in the frequency range from 0.76 f_{NL} to 1.3 f_{NL}. Above the latter frequency, RSR_{NL-L} shows greater variability (the standard deviation is about three times larger); on average however, the non-linear response remains significantly smaller than the linear one, with a minimum value of 0.5 and a high frequency asymptote around 0.8.

The large variability above f_{NL} can be partially explained by a few specific cases displaying specific non-linear soil behaviour. We find 10 sites with a RSR_{NL-L} amplitude exceeding 1 at some frequency beyond f_{NL}: AKTH04, IBRH16, IWTH02, IWTH03, IWTH26, KRSH05, MYGH10, SZOH37, TCGH10, AKTH14. A possible explanation of this observation, as proposed by several authors (Bonilla et al., 2005; Frankel et al., 2002; Roten et al., 2013) reporting similar behaviors on some sites, is related to pore water pressure build up during seismic loading, with proximity to liquefaction.

The "extreme" values of RSR_{NL-L} obtained for all subsets are given in Table 1. By extreme values we mean the largest values in the low frequency part ($f < f_{NL}$), for both the average and average + one standard deviation, the smallest average and average – one standard deviation in the high-frequency part ($f > f_{NL}$), together with the largest average + one standard deviation value in the same high frequency part. Although not shown here, the same trends are observed for the two other subsets with different PGA threshold values. As expected, for lower PGA threshold values, the maximum RSR_{NL-L} amplitude at low frequency decreases (from 1.6 for 300cm/s^2 to 1.4), while the minimum RSR_{NL-L} amplitude at high frequency increases (from 0.5 for 300cm/s^2 to 0.6 for 100cm/s^2).

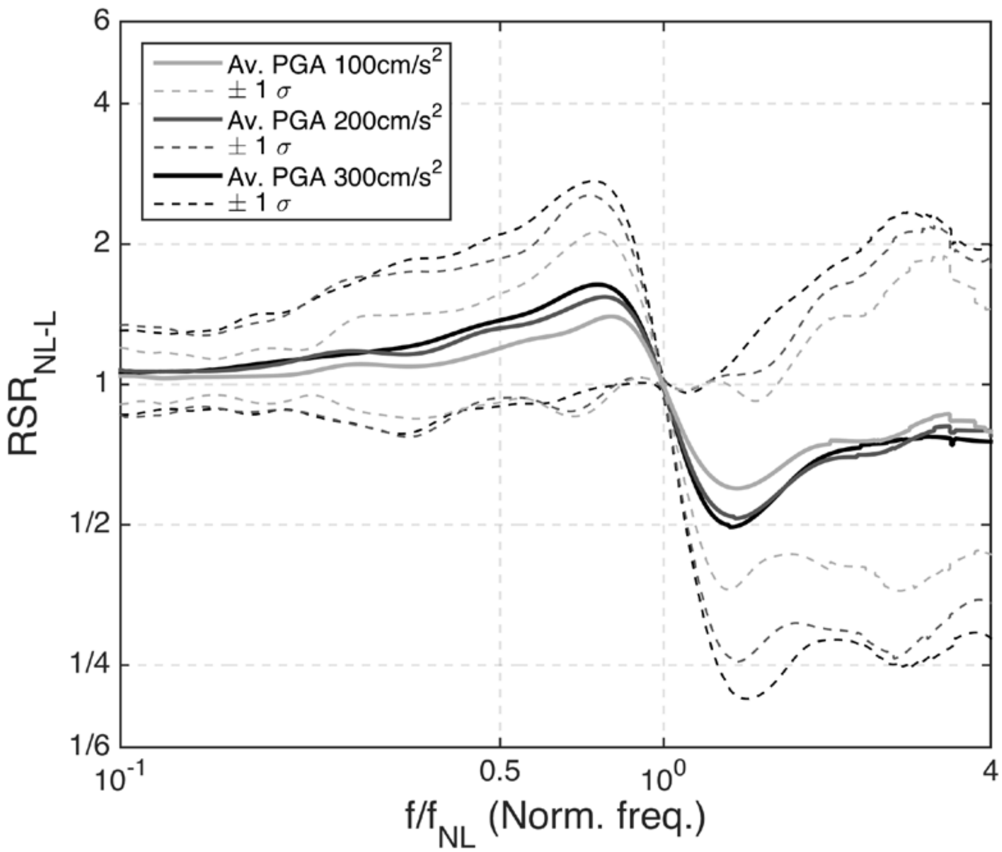

Fig. 3 –Average RSR_{NL-L} curves displayed as a function of the dimensionless frequency axis (f/f_{NL}), for the 35 sites common to the 3 subsets. The different sets of curves correspond to three different PGA thresholds (black = 300 cm/s^2, grey = 200 cm/s^2, light grey = 100 cm/s^2). The solid line is for the average curve, the dashed lines for the average ± one standard deviation.

Table 2 – Statistics on the normalized RSR_{NL-L} values for the three different subsets for the 35 common sites.

	freq<f_{NL}. mean value	freq<f_{NL} Mean +1σ	freq>f_{NL} mean value	freq>f_{NL} Mean -1σ	freq>f_{NL} Mean +1σ
Subset 1 (PGA>100 cm/s^2)	1.4	2.1	0.6	0.4	1.9
Subset 2 (PGA >200 cm/s^2)	1.5	2.5	0.5	0.3	2.2
Subset 3 (PGA >300 cm/s^2)	1.6	2.7	0.5	0.2	2.4

5. Conclusions

We characterize non-linear effects on site response by computing the ratio between the site responses for strong and weak motions (RSR_{NL-L}). The shape of this curve is divided into three main parts, consisting of a low frequency part with an amplitude above 1 (the strong motion site response exceeds the weak motion one), a high frequency part with an amplitude significantly lower than 1 (the strong motion response is decreased with respect to the weak motion one), separated by a transitional part around a site-specific transition frequency f_{NL}.

We normalized each RSR_{NL-L} frequency curves by the corresponding f_{NL} values and computed an average RSR_{NL-L} curve for all sites and for 3 different values of the PGA threshold defined for selecting strong events. The amplitude of the RSR_{NL-L} curve is found to depend on the PGA threshold value, while f_{NL} exhibit only a very slight dependency on PGA threshold (with the exception of a few sites). The peak low frequency amplitudes are 1.4, 1.5 and 1.6, and the minimum, high frequency amplitudes are 0.6, 0.5 and 0.5, for selected PGA threshold values of 100, 200 and 300 cm/s^2, respectively.

The non-linear soil behavior has significant effects on the average site response, even for a relatively moderate PGA threshold value of 100 cm/s^2. There is a significant decrease of the amplification above 10 Hz.

The low-frequency amplification increase (below f_{NL}) is found to be a quasi-systematic consequence of the non-linear soil behaviour, and should be emphasized, as it is not reported in any other article, and can be significant (up to a factor of 1.5). On the other hand, the high-frequency amplification decrease is well documented in the literature. Most studies report de-amplification factors ranging between 0.6 and 0.15. Our observations show that the average observed values are about 0.5, though it may reach much lower values in some narrow frequency bands. Nevertheless, for a few sites, the non-linear soil behavior may lead to increased high-frequency amplification, as often reported in previous studies and mostly explained by pore water pressure and cyclic mobility.

6. Data and resources

Time histories and velocity profiles used in this study were collected from the KiK-net web site: www.kik.bosai.go.jp and www.kik.bosai.go.jp/kik/ (last accessed October 2014).

7. Acknowledgments:

Part of the work realized in this paper has been carried out with French funding managed by the National Research Agency under the program "Future Investments" (SINAPS@ project, reference No. ANR-11-RSNR-0022; SINAPS@ is a SEISM Institute project, see http://www.institut-seism.fr/en/) We also want to thanks Marianne Marot for her review, James Kaklamanos and an anonymous reviewer for their precious comments and advices.

References

[1] Aguirre, J., Irikura, K., 1997. Nonlinearity, Liquefaction, and Velocity Variation of Soft Soil Layers in Port Island, Kobe, during the Hyogo-ken Nanbu Earthquake. Bull. Seismol. Soc. Am. 87, 1244–1258.

[2] Assimaki, D., Li, W., 2012. Site and ground motion-dependent nonlinear effects in seismological model predictions. Soil Dyn. Earthq. Eng. 143–151.

[3] Bard, P.-Y., Bouchon, M., 1985. The two-dimensional resonance of sediment-filled valleys. Bull. Seismol. Soc. Am. 75, 519–541.

[4] Beresnev, I.., Wen, K.., 1996. Nonlinear soil response, A reality? Bull. Seismol. Soc. Am. 86, 1964–1978.

[5] Bolisetti, C., Whittaker, A. S., Mason, H. B., Almufti, I., Willford, M., 2014. Equivalent linear and nonlinear site response analysis for design and risk assessment of safety-related nuclear structures. Nuclear Engineering and Design, 275, 107-121.

[6] Bonilla, L.F., Archuleta, R.J., Lavallée, D., 2005. Hysteretic and Dilatant Behavior of Cohesionless Soils and Their Effects on Nonlinear Site Response: Field Data Observations and Modeling. Bull. Seismol. Soc. Am. 95, 2373–2395.

[7] Bonilla, L.F., Tsuda, K., Pulido, N., Regnier, J., Laurendeau, A., 2011. Nonlinear site response evidence of K-net and KiK-net records from the Mw 9 Tohoku earthquake. Earth Planets Space 58.

[8] Cadet, H., Bard, P.-Y., Duval, A.-M., Bertrand, E., 2012. Site effect assessment using KiK-net data: part 2—site amplification prediction equation based on f0 and Vsz. Bull. Earthq. Eng. 10, 451–489.

[9] Choi, Y., Stewart, J.P., 2005. Nonlinear site amplification as function of 30 m shear wave velocity. Earthq. Spectra 21, 1–30.

[10] Drouet, S., 2006. Analysis of the accelerometric data applied to seismic hazard assessment in France. Université toulouse III-Paul Sabatier.

[11] Duval, A.-M., Bard, P.-Y., Méneroud, J.-P., Vidal, S., 1996. Mapping site effect with microtremors, in: International Conference on Seismic Zonation. pp. 1522–1529.

[12] Field, E., Johnson, P.A., Beresnev, I.A., Zeng, Y., 1997. Nonlinear ground-motion amplification by sediments during the 1994 Northridge earthquake. Lett. Nat. 599–602.

[13] Frankel, A.D., Carver, D.L., Williams, R.A., 2002. Nonlinear and Linear Site Response and Basin Effects in Seattle for the M 6.8 Nisqually, Washington, Earthquake. Bull. Seismol. Soc. Am. 92, 2090–2109.

[14] Fujiwara, H., Aoi, S., Kunugi, T., Adachi, S., 2004. Strong-motion Observation Networks of NIED: K-NET and KiK-NET. National Research Institute for Earth Science and Disaster Prevention.

[15] Kaklamanos, J., Baise, L.G., Thompson, E.M., Dorfmann, L., 2015. Comparison of 1D linear, equivalent-linear, and nonlinear site response models at six KiK-net validation sites. Soil Dyn. Earthq. Eng. 69, 207–219.

[16] Kaklamanos, J., Bradley, B.A., Thompson, E.M., Baise, L.G., 2013. Critical Parameters Affecting Bias and Variability in Site‐Response Analyses Using KiK‐net Downhole Array Data. Bull. Seismol. Soc. Am. 103, 1733–1749.

[17] Kaklamanos, J., Bradley, B. A., 2015. Evaluation of 1D nonlinear total-stress site response model performance at 114 KiK-net downhole array sites. Proceedings of the 6th International Conference on Earthquake Geotechnical Engineering 1-4 November 2015 Christchurch, New Zealand, paper # 278, 9 pages.

[18] Kim, B., Hashash, Y.M., 2013. Site response analysis using downhole array recordings during the March 2011 Tohoku-Oki earthquake and the effect of long-duration ground motions. Earthq. Spectra 29, S37–S54.

[19] Kokusho, T., 2004. Nonlinear site response and strain-dependent soil properties. Curr. Sci. 87, 1363–1369.

[20] LeBrun, B., Hatzfeld, D., Bard, P.Y., 2001. Site effect study in urban area: Experimental results in Grenoble (France),. Pure Appl. Geophys. 158, 2543–2557.

[21] Noguchi, S., Sasatani, T., 2008. Quantification of Degree of Nonlinear Site Response, in: The 14th World Conference on Earthquake Engineering, Beijing, China.

[22] Régnier, J., Bonilla, L.F., Bertrand, E., Semblat, J.-F., 2014. Influence of the VS Profiles beyond 30 m Depth on Linear Site Effects: Assessment from the KiK-net Data. Bull. Seismol. Soc. Am. 104, 2337–2348.

[23] Régnier, J., Cadet, H., Bonilla, L.., Bertand, E., Semblat, J.F., 2013. Assessing nonlinear behavior of soil in seismic site response: Statistical analysis on KiK-net strong motion data. Bull. Seismol. Soc. Am. 103, 1750–1770.

[24] Régnier, J., Cadet, H.,Bard P.Y. Empirical quantification of the effects of non-linear soil behaviour on site response. Accepetd in BSSA in May 2016.

[25] Roten, D., Fäh, D., Bonilla, L.F., 2013. High-frequency ground motion amplification during the 2011 Tohoku earthquake explained by soil dilatancy. Geophys. J. Int. 193, 898–904.

[26] Rubinstein, J. L., 2011. Nonlinear site response in medium magnitude earthquakes near Parkfield, California. Bulletin of the Seismological Society of America, 101(1), 275-286.

[27] Sandikkaya et al., 2013

[28] Sandikkaya, M. A., Akkar, S., Bard, P. Y., 2013. A nonlinear site-amplification model for the next pan-European ground-motion prediction equations. Bulletin of the Seismological Society of America, 103(1), 19-32.

[29] Satoh, T., Sato, T., Kawase, H., 1995. Nonlinear Behavior of Soil Sediments Identified by Using Borehole Records Observed at the Ashigara Valley, Japan. Bull. Seismol. Soc. Am. 85, 1821–1834.

[30] Steidl, J.H., Tumarkin, A.G., Archuleta, R.J., 1996. What is a reference site? Bull. Seismol. Soc. Am. 86, 1733–1748.

[31] Walling, M., Silva, W., & Abrahamson, N. (2008). Nonlinear site amplification factors for constraining the NGA models. Earthquake Spectra, 24(1), 243-255.

[32] Wen, K.-L., Huang, J.-Y., Chen, C.-T., Cheng, Y.-W., 2011. Nonlinear site response of the 2010 Darfield, New Zealand earthquake sequence, in: 4th IASPEI / IAEE International Symposium: Effects of Surface Geology on Seismic Motion.

[33] Yee, E., Stewart, J.P., Tokimatsu, K., 2013. Elastic and large-strain nonlinear seismic site response from analysis of vertical array recordings. J. Geotech. Geoenvironmental Eng. 139, 1789–1801.

[34] Yu, G., Anderson, J.G., Siddharthan, R., 1993. On the characteristics of nonlinear soil response. Bull. Seismol. Soc. Am. 83, 218–244.

[35] Zalachoris, G., Rathje, E.M., 2015a. Evaluation of One-Dimensional Site Response Techniques Using Borehole Arrays. J. Geotech. Geoenvironmental Eng. 04015053.

[36] Zalachoris, G. and E. M. Rathje, 2015b. Comparisons of One-Dimensional Site Response Analysis and Borehole Array Observations: Quantification of Bias and Variability. Proceedings of the 6th International Conference on Earthquake Geotechnical Engineering, 1-4 November 2015 Christchurch, New Zealand, paper # 128, 9 pages.